FEA Analysis and Experimental Investigation of Building Blocks for Flexural Mechanism

Rachel Patil[1], Suhas Deshmukh[2], Y.P. Reddy[3], Kavidas Mate[4]
Department of Mechanical Engineering
[1,3]Sinhgad College of Engineering, Vadgaon
[2,4]Sinhgad Academy of Engineering, Kondhwa
Pune, India
[1]rachelpatil@gmail.com, [2]suhas.deshmukh@gmail.com

***Abstract*— Planar XY Flexural Mechanisms have numerous applications in precision motion mechanisms. Flexural mechanisms generate relative motion between fixed support and motion stage using flexibility of material. This type of mechanisms offers frictionless motion, zero backlash and high order of repeatability. Flexural mechanisms consist of motion stage, flexible elements (building blocks) and fixed support. Various researchers developed flexural mechanism using various building blocks; these can be broadly categorized into hinges and planar type. Present paper investigates basic building blocks of planar flexural mechanism such as single cantilever beam, parallelogram flexure and double parallelogram flexure based on various performance parameters such as deformation, stiffness, payload capacity, parasitic error, angular rotation and cross axis coupling error etc. using FEA analysis tool ANSYS. It is observed that Double Parallelogram Flexural Manipulator (DFM) offers better performance, hence experimental setup is developed using DFM. Comparison of different building blocks of flexural mechanism shows DFM offers better performance and is further experimentally validated. Also, FEA analysis of XY Flexural mechanism which uses DFM as building block is presented.**

***Keywords*—** Flexural Mechanism, Parametric Modeling, Double Flexural Manipulator (DFM), dSPACE DS1104

I. Introduction

A novel piezo-driven, parallel-kinematic, micro positioning XY stage of monolithic design comprised of parallelogram four-bar linkages, flexure hinges, and piezoelectric actuators shows that the mechanical structure of the stage has a large work space, high bandwidth and good linearity [1, 2]. The development of a novel compact high precision XY-scanner providing nanometre-level resolution and millimeter-level working range provides the optimal trade-off in terms of design variables. The scanner is composed of a voice coil motor (VCM) and double compound linear spring flexure guide mechanisms to satisfy both accuracy and travel range specifications, and to reduce parasitic motion during scanning [3]. A parallelogram mechanism with flexure hinges, lever mechanisms and piezoelectric actuators has been designed to make XY-displacement in monolayer plane structure. The area efficiency and volume efficiency of piezo driven XY-micro-stage are very higher than electrostatic driven and electromagnetic driven one [4].

A planar 3-DOF parallel-type micro positioning mechanism is proposed in consideration of accurate flexure hinge modeling. More precise modeling of the flexure hinge mechanism is necessary to enhance the positional accuracy of Microsystems. This device can be usefully employed for SEM, x-ray lithography, mask alignment, micromachining, and other similar technologies [5]. A novel long-travel piezoelectric-driven linear nano-positioning device provides a valuable tool for micro/nano measurement equipment applications [6, 14]. The demands of ultra-high-precision positioning stages are continuously increasing. The current nanotechnology requires nano-manipulation stages that can move and position the specimen to various locations and in desired orientations. This motion needs to be in multiple DOFs with long travel ranges at nano-scale resolution [11, 12, 13].

Flexural mechanisms have recently been used in increasingly many applications and have come under a lot of analysis. Some of the basic design issues involved in the fabrication of small length flexure mechanisms have been treated previously. Researchers have also studied various kinds of flexures for obtaining rotational motion from the point of view of optimal force transmission. An application of some of these general principles to a novel fabrication technology was developed at UC Berkeley during the Micromechanical Flying Insect (MFI) project. This technique is ideally suited to fabricating mechanisms at the millimeter scale [7]. The purpose of synthesis of the technical results obtained in the frame of the HAFHA (High Accuracy Flexural Hinge Assembly) development has been made to develop a competitive technology for a flexural pivot, usable in highly accurate and dynamic pointing/scanning mechanisms. Compared with other solutions (e.g. magnetic or ball bearing technologies) flexural hinges are the appropriate technology for guiding with accuracy a mobile payload over a limited angular ranges around one rotation axis [8]. Phonosurgery has to do with a surgical procedure, performed with an aim to enhance the

978-1-4799-7263-0/15/$31.00 ©2015 IEEE

voice. Common anomalies of the vocal fold include a wide variety of pathologies such as nodules, polyps, cysts, and cancer. The method most commonly used of phonosurgery is done using a laser beam. The laser beam source is located approximately forty centimeters away from the vocal cords. With this long distance, a small accuracy error would strongly impact the quality of the intervention. Recent advances in the area of micro mechanisms used in medicine have increased the potential for an early detection and a better treatment against vocal folds diseases Using microdevices, micromechanisms can be designed to guide the laser beam nearest to the vocal fold, for an accurate treatment and for minimizing the risk of detriment of the delicate vocal fold structures [9]. Also the use of compliant mechanisms constitutes a very promising option for shape adaptable airfoil structures.

With all these wide range of applications, flexural mechanisms can be successfully used for wide range of macro, micro and nano scales. A two DOF planar mechanism basically constitutes of building blocks; the simple beam flexure, the parallelogram flexure and the double parallelogram flexure. This paper presents the FEA analysis and comparison of these building blocks with respect to displacement, rotation and parasitic motion to obtain an error free flexural mechanism. It also aims in performance evaluation of proposed XY flexural mechanism fabricated with optimum designed values.

II. Flexural Mechanism

Flexural mechanism gives precision motion by having relative motion between fixed support and motion stage. Relative motion is generated by interface element as shown in Fig. 1. An interface element such as ball bearings, sliders, and liquid / air films used in conventional mechanisms generate friction, backlash and do not offer high precision and high order of repeatability. If these interface elements are replaced with flexible elements such as hinges, flexible beams eliminates friction, backlash and offers high precision scanning with high order of repeatability. Based on this basic principle XY, XYθ, etc. flexural mechanisms are developed. Investigation of these building blocks of flexural mechanism is very important to achieve desired motion objectives. Hence present paper investigates different planar flexural building blocks and presented in next section.

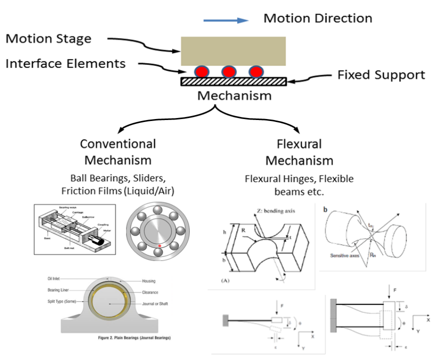

Fig. 1 Concept of Mechanism and Interface Elements

III. Basic Building Blocks of Flexural Mechanism

In this section various planar flexural building blocks are analyzed using FEA tool. The feature-based parametric modeling technique (shown in Fig. 2) from ANSYS is used. Initial geometry is created using DesignModeler, DesignModeler has feature to define parameters such as length, width and thickness etc. of geometry. Such parametric model is further considered for FEA analysis where boundary conditions are applied and results are evaluated. The word parametric means the geometric parameters can be varied in the design process and output pefromance can be evaluated with respect to this parametric variation. Parametric modeling is accomplished by identifying and creating the key features of the design. FEA Analysis and its results for single beam flexure, parallelogram flexure and double parallelogram flexure is presented in next subsections

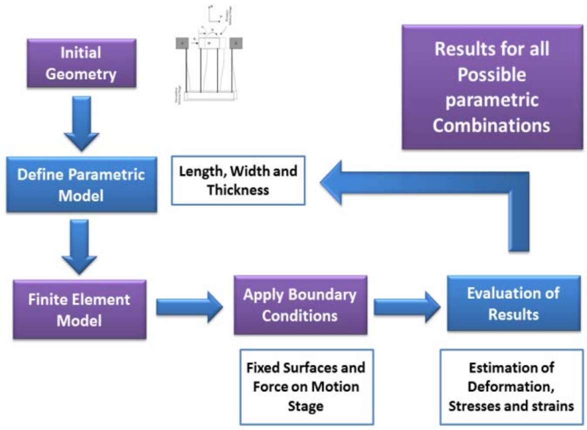

Fig. 2 Parametric FEA Analysis Procedure

A. Single Beam Flexure

Simple beam is used as a building block in the XY flexural mechanisms (shown in Fig.3). From beam bending analysis we know that there is deflection of beam tip (δ) in the direction of force. Also the tip rotates (θ) and moves in X-direction called parasitic motion which is not desirable.

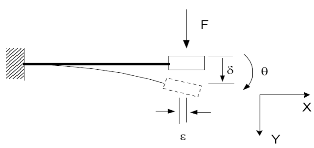

Fig. 3 Single Beam Flexure [1]

Theoretically, deflection, parasitic motion and angular rotation are calculated by,

$$\delta = \frac{FL^3}{3EI} \qquad \theta = \frac{FL^2}{2EI} \qquad \varepsilon \approx \frac{\delta^2}{L} \qquad (1)$$

Deflection, angular rotation and parasitic error motion of cantilever beam depends on geometric parameters as well as material properties. Hence parametric model for cantilever beam is developed using DesignModeler which varies input parameters such as length, width and thickness of the beam.

Parametric modeling and FEA analysis is carried out using ANSYS. For a cantilever beam (L=50mm W=15mm T=0.5mm) static structural analysis is carried out and deformation of 11.292 mm is observed under 1 N bending force (Fig. 4). Deformations and stresses depends on geometric as well as material properties, hence to achieve appropriate stiffness for the building block we need to vary the length, width and thickness of the cantilever beam. Hence parametric model (from ANSYS 14.5) approach is used to observe the variation of deformation, stress with varying geometric parameters.

Range of beam for parametric modeling is lengths 50mm, 75mm, 100mm and 125mm; widths equal to 5mm, 10mm, 15mm to 20mm and thickness ranging from 0.5 to 1mm. Fig. 5 & 6 shows a variation of deformation and von-mises stress with parameters (Length, Width and Thickness). It is observed that variation of Deformation, Von-mises stresses is non-linear with respect to change in thickness, width and length of beam

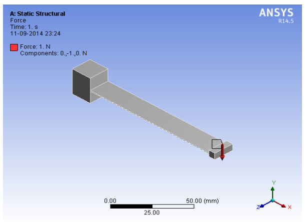

Force = 1N (-Y)

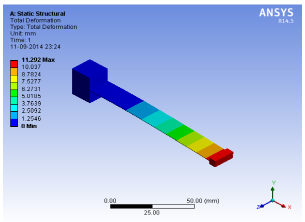

Maximum Deformation = 11.292 mm

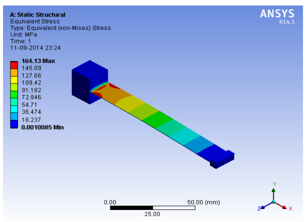

Equivalent Von-mises Stress = 164.13 MPa

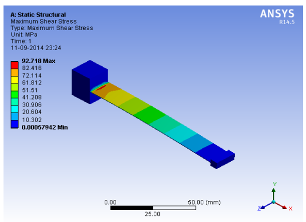

Maximum Shear Stress = 92.718 MPa

Fig. 4 Analysis of a Cantilever beam flexure

Using similar approach other building blocks of flexural mechanisms such as parallelogram and double parallelogram flexure is analyzed and presented.

B. Parallelogram Beam Flexure

The parallelogram flexure unit also suffers from undesirable parasitic errors (Fig. 7). An application of force in the Y direction results in the desired motion δ, in Y direction, and also in undesired motions ε in the negative X direction, and rotational twist θ. The accuracy is better but nevertheless undesired motions still exist. In-plane rotation of the Motion Stage in constrained quite well because the parallelogram flexure unit is considerably stiff in rotation.

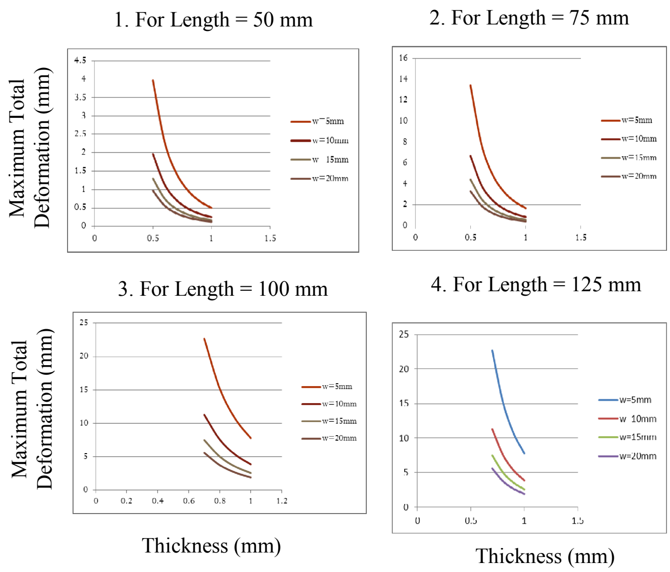

Fig. 5 Variation of deformation Vs thickness of beam for parametric analysis of a cantilever flexural beam

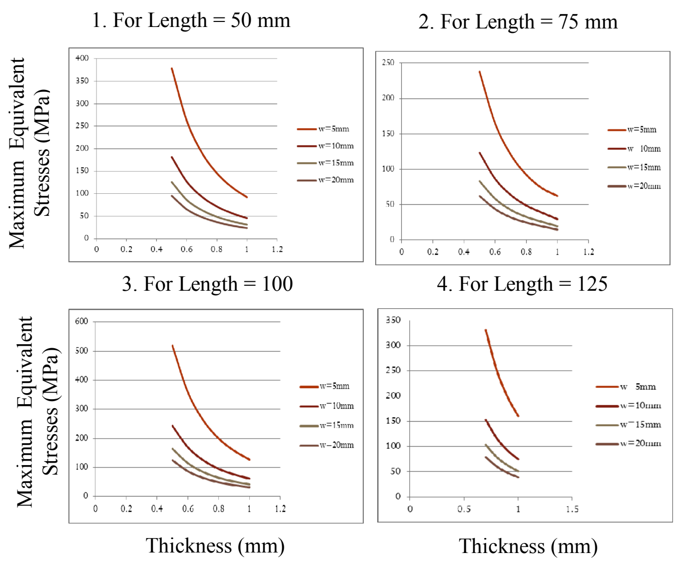

Fig. 6 Variation of Maximum Von-mises stresses Vs thickness of beam of a cantilever flexural beam

$$\delta = \frac{FL^3}{24\,EI} \qquad \theta \approx 2\left(\frac{t}{b}\right)^2 \frac{\delta}{L} \qquad \varepsilon \approx \frac{3\delta^2}{5L}$$

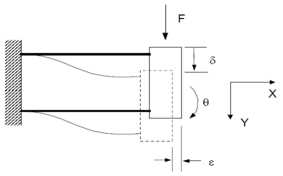

Fig. 7 Parallelogram Beam Flexure

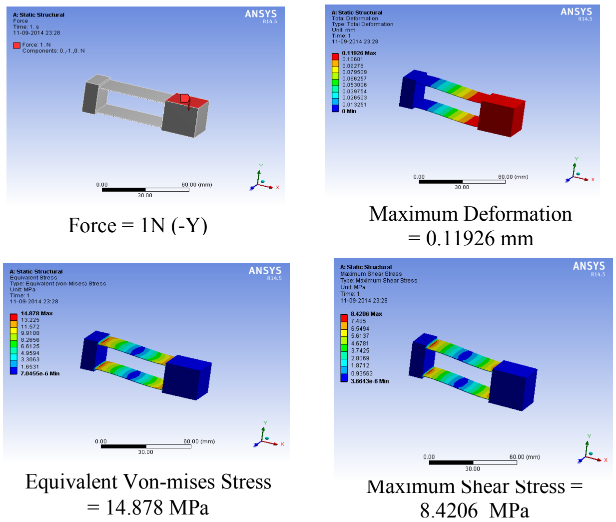

Fig. 8 Analysis of a parallelogram beam flexure

Parametric modeling is carried out same as in cantilever beam for lengths 50mm, 75mm, 100mm and 125mm; widths equal to 5mm, 10mm, 15mm to 20mm and thickness ranging from 0.5 to 1mm (Fig. 8). The variations in deformation and von-mises stress with respect to width and thickness are as shown in Fig. 9 and Fig. 10 respectively.

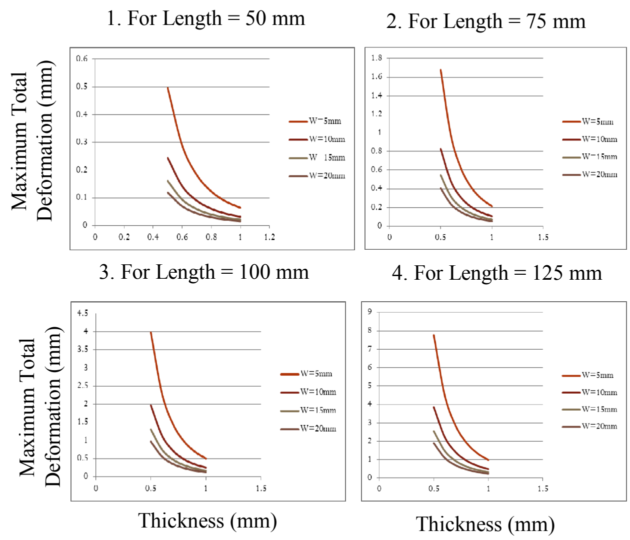

Fig. 9 Graphs of deformation Vs thickness of beam for parametric analysis of a parallelogram beam flexure

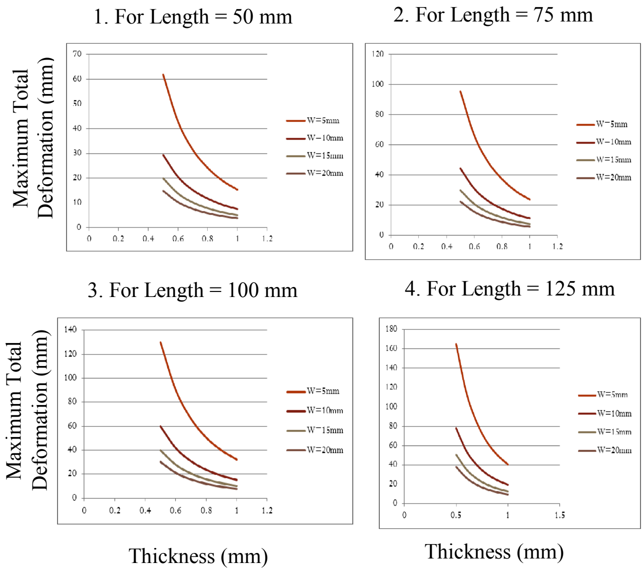

Fig. 10 Graphs of Equivalent Von-mises stresses Vs thickness of beam for Parallelogram Beam Flexure

C. Double Parallelogram Flexure

The double parallelogram flexure unit is used as the building block for two-axis planar flexural mechanisms (Fig. 11) which is also called Double Flexural Mechanism (DFM).

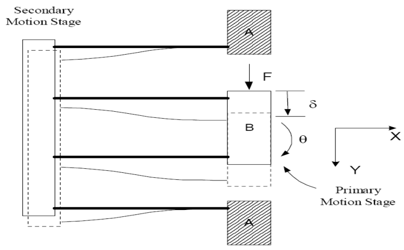

Fig. 11 Double Parallelogram Beam Flexure

Deflection, Angular rotation and parasitic error motion is calculated by

$$\delta = \frac{FL^3}{12\,EI} \qquad \theta \approx t^2\left(\frac{1}{b_1^2}+\frac{1}{b_2^2}\right)\frac{\delta}{L} \qquad \varepsilon = 0$$

Fig. 12 shows analysis of DFM for force 1N in Y direction causes a deformation of 9.785mm; von-mises stresses 97.943MPa and shear stresses 55.146 MPa as shown in Fig. 12. Analysis shows that this flexure allows relative Y translation between bodies A and B, but is stiff in relative X displacement and rotation, although not as stiff as the parallelogram flexure. The parasitic error ε, along X direction, is considerably smaller because any length contraction due to beam deformation is absorbed by a secondary motion stage.

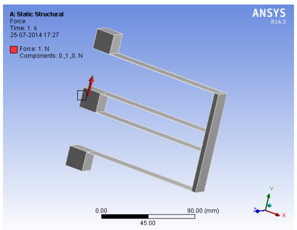

Force applied = 1N

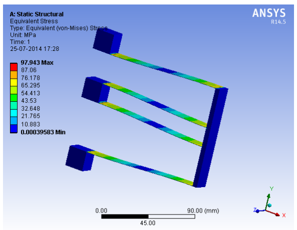

Equivalent Von-mises Stress = 97.943 MPa

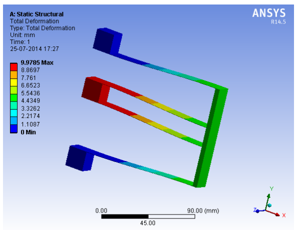

Maximum Deformation = 9.9785 mm

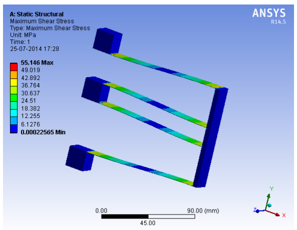

Maximum Shear Stress = 55.146 MPa

Fig. 12 Analysis of a Double parallelogram beam flexure

There exist rotational parasitic motions, which may be eliminated by appropriate location of the Y direction force (Actuator placement). Hence, body A exhibits pure Y-translation with respect to body B on the application of a Y direction force. Hence performance of DFM is better compared to other two flexure blocks. Further similar parametric analysis of DFM manipulator is carried out and Fig. 13 and 14 shows deformation, stress analysis results. Next section presents comparison of flexure blocks based on parasitic error and angular rotation.

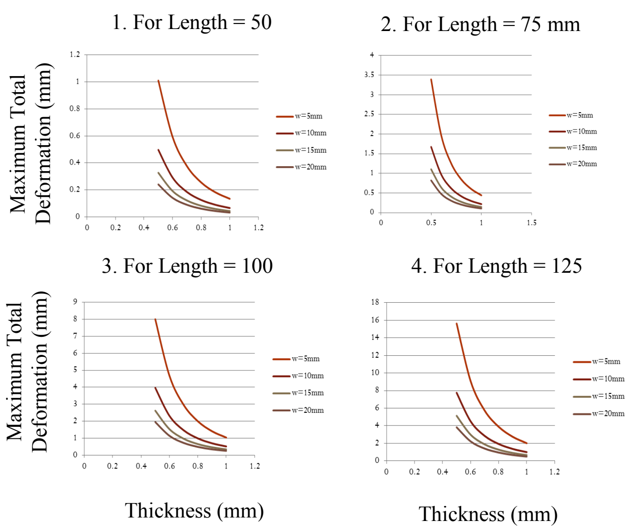

Fig. 13 Graphs of deformation Vs thickness of beam for parametric analysis of Double Parallelogram Flexural Mechanism

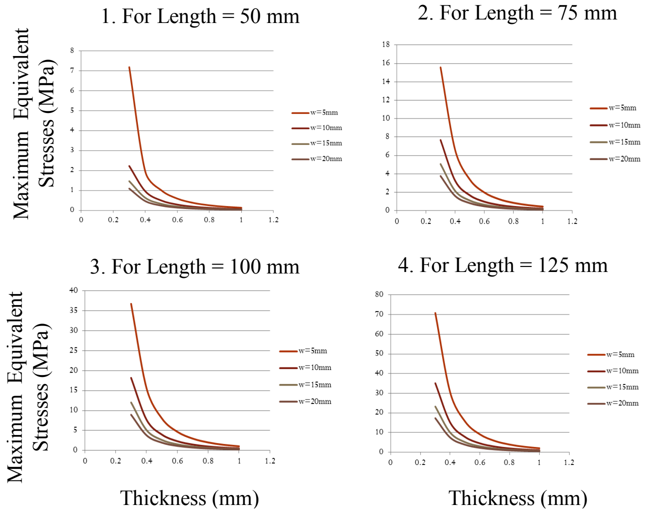

Fig. 14 Graphs of Equivalent Von-mises stresses Vs thickness of beam for Double Parallelogram Flexural Mechanism

D. Comparison of Building Blocks

Since the primary objective of the XY mechanisms is to provide guided motion along X and Y directions, and constrain all other motions, it is desirable to maintain the high stiffness and small parasitic errors. In other words, the degrees of constraints should be as close to ideal as possible. In the above text we have discussed three different flexures which can be used as building blocks for XY mechanisms.

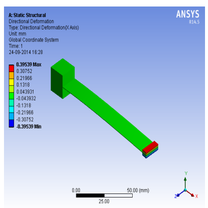
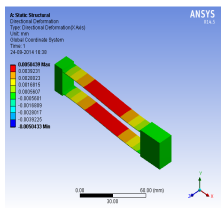
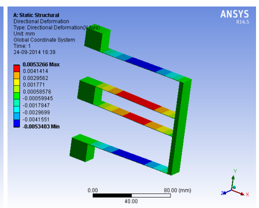

Fig. 15 FEA Analysis Results of Parasitic Error Motion in Cantilever beam, Parallelogram Flexure and Double parallelogram Flexural Mechanism

Table No. 1: Comparison of building blocks with respect to deformation, parasitic error and angular rotation (* Deformation of all flexural building blocks are not same as their stiffness are different. Hence parasitic error motion and angular rotation are calculated based on percentage with respect to deformation)

Parameter	**Cantilever Beam**	**Parallelogram Flexure**	**Double Flexure Mechanism**
Deformation (δ mm)	10.5013499	1.301827458	2.620780755
Parasitic Error (ε mm)	0.395385 ***(3.76 %)****	0.005043 ***(0.387%)****	0.00532659 ***(0.2032%)****
Angular Rotation (θ)	2.16 ***(20.56%)****	0.23 ***(17.66%)****	0.12 ***(4.57%)****

These three building blocks cantilever beam, parallelogram flexural beam and double flexural mechanism are compared with respect to deformation, parasitic error and angular rotation for length 100 mm, width 15 mm and thickness 0.5

mm shown in Table No.1. It is observed that DFM gives minimum parasitic error and negligible angular rotation as compared to the other two flexures and thus can be successfully used to form an XY mechanism.

IV. EXPERIMENTAL SETUP OF DFM

Fig. 17 shows the experimental set-up of DFM manipulator. Various values for maximum deformation, parasitic error and stresses are estimated experimentally. DFM consists of actuator (VCM), sensor (Optical Encoder with 50nm resolution) and further connected to PC via dSPACE microcontroller. MATLAB Simulink code was developed to impart a force of known amount to motion stage and acquire the position signal of motion stage. Experimental measurements are carried out to estimate force deflection characteristics of the DFM.

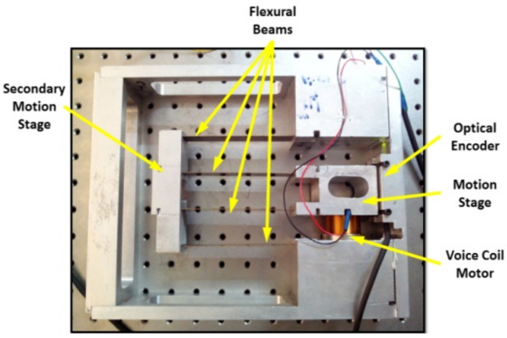

Fig. 16 Manufactured Single Stage DFM Manipulator

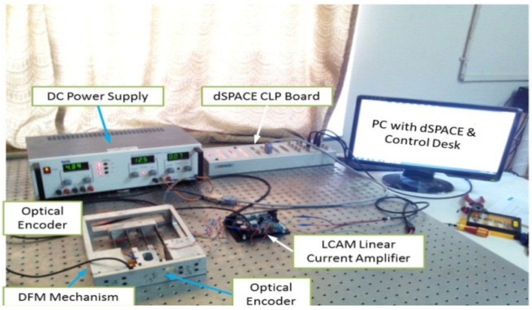

Fig. 17 Experimental Setup of Sensor-less DFM (Double Flexural Manipulator)

Table No.2 shows the experimental verification of deflection and parasitic error with the evaluated theoretical value and values of FEA analysis. According to present requirement of operation (In the current work, a parametric study to investigate the required dimensions for the double flexural manipulator has been conducted. The load in the current study was a direct force of 5 N which produced a deflection of 10mm.), mechanism dimensions are finalized as below: It can be observed that the required deflection of $\pm$10 mm is to be obtained. For length=100 mm, width=20 mm, and thickness=0.5mm gives a 9.968 mm deformation and stresses are within the elastic limit ($\sigma = 268\ N/mm^2$, $\sigma_{ut} = 500\ N/mm^2$).

Table No. 2 : Experimental Verification of deflection and parasitic error

Force (N)	Deflection (mm)			Parasitic error (experimental)	(%) Error (Theoretical)	(%) Error (FEA)
	Theoretical	Experimental	FEA			
-5	-7.692	-7.73	-8.2131	0.0253	0.49	0.4831
-2.5	-3.846	-3.874	-3.8755	0.0352	0.724	0.0015
2.5	3.846	3.877	3.8755	0.0435	0.802	0.0015
5	7.692	7.711	7.7511	0.0567	0.243	0.0401

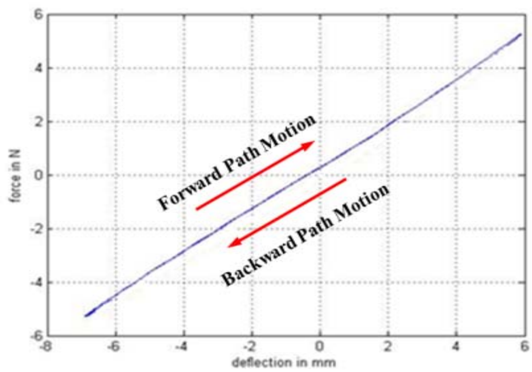

(a) Experimental Estimation of Stiffness of DFM Mechanism

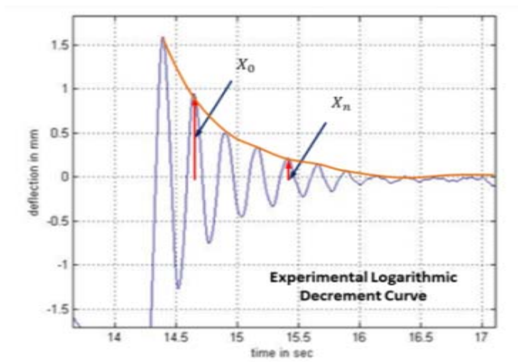

(b) Experimental Step Response of DFM Mechanism

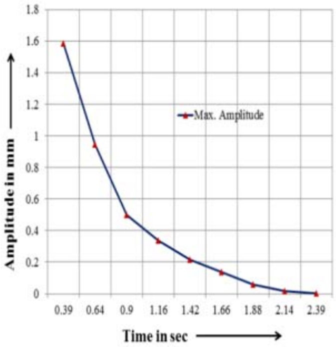

Time in sec	Max. Amplitude in mm
0.39	1.586
0.64	0.945
0.9	0.4997
1.16	0.3352
1.42	0.215
1.66	0.1391
1.88	0.05985
2.14	0.0172
2.39	0.002

(c) Experimental Logarithmic Decrement Curve for DFM Mechanism

Figure 18 Experimental Investigation of DFM

Various mechanical properties like Stiffness, damping factor etc also estimated precisely using the DFM. Natural frequency of the system is also estimated of the set-up.

Stiffness Estimation: Stiffness (slope of experimental force deflection curve) is determined. MATLAB Simulink code was developed to command the actuator and position of motion stage is measured using installed optical encoder. Stiffness is experimentally evaluated in both forward and backward motion. Fig. 7 shows experimental force and deflection of motion stage of DFM Mechanism.

Damping Factor Estimation: Motion stage is given an initially displacement by a momentary force and then allowed to vibrate freely till it comes to a halt. Experimental results (see Fig. 8 & 9) is obtained and plotted as deflection vs time. Concept of Logarithmic decrement is further used for the calculation of damping factor. Logirithmic decrement is given by,

Logarithmic decrement

$$\delta = \frac{1}{n}\left[\log\left(\frac{X_n}{X_m}\right)\right]$$

Damping Factor

$$\xi = \frac{\delta}{\sqrt{4\pi^2 - \delta^2}}$$

From above experimental results logarithmic decrement and damping factor in DFM mechanism is calculated as below,

$$\delta = 0.218308; \quad and \quad \xi = 0.034785$$

Estimated natural frequency of DFM is 24.51 rad/s or 3.90 Hz this is in close agreement with FEA Modal analysis of DFM Mechanism. DFM gives better performance characteristics as compared to other building blocks of mechanism. XY Flexural mechanism using DFM (which is presented in Awatar's thesis [1]) is analyzed and presented in next section.

V. XY Flexural Mechanism

Double parallelogram flexure offers large range, good rotational stiffness, no purely kinematic parasitic errors, and excellent thermal stability. The standard double parallelogram flexure module is used as a building-block and various XY planar flexural mechanisms are developed by Awatar [1]. FEA analysis of one of the mechanism is carried out in this section. Fig. 19 shows a planar flexural mechanism [1], which uses DFM as building block.

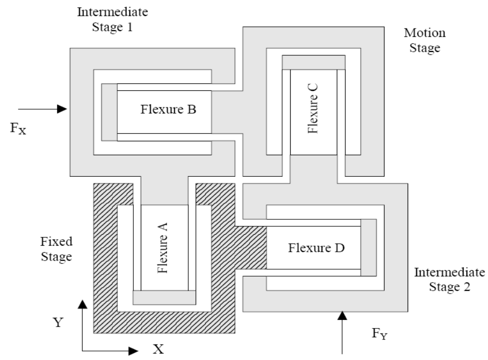

Fig. 19 XY Flexural Mechanism

The primary objective of the design is to achieve large ranges of motion along the X and Y. In design it is the need to maintain high stiffness and small error motions in the out-of-plane directions. The mechanism is so designed such that the rotation of the motion stage, being a parasitic error motion, is inherently constrained.

The above mechanism shown in Fig. 19 achieves all the desirable attributes required in XY mechanism. The constraint arrangement includes four basic rigid stages: Ground, Motion Stage, and intermediate Stages 1 and 2. Stage 1 is connected to ground by means of flexure module A, which only allows relative X translation; the Motion Stage is connected to Stage 1 via flexure module B, which only allows relative Y translation; the Motion Stage is connected to Stage 2 via flexure module C, which only allows a relative X translation; and finally, Stage 2 is connected to Ground by means of flexure module D, which only allows relative Y translation. Thus, in any deformed configuration of the mechanism, Stage 1 will always have only an X displacement with respect to Ground while Stage 2 will have only a Y displacement. Furthermore, the Motion Stage inherits the X displacement of Stage 1 and the Y displacement of Stage 2, thus acquiring two translational degrees of freedom that are mutually independent. Since the Y and X displacements of the Motion Stage do not influence Stage 1 and Stage 2, respectively, these are ideal locations for applying the actuation loads

FEA analysis is carried out to estimate maximum deformation, von-mises stresses and shear stresses and is as shown in Fig. 20 and Fig. 21. Force is applied in X and Y direction respectively. The deformation observed along cross axis is negligible (shown in Fig. 22).

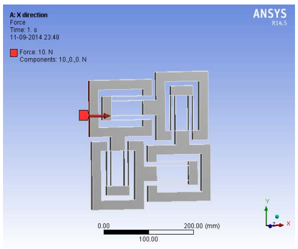

Force applied = 1N (X)

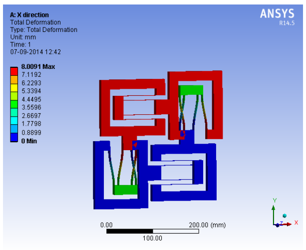

Max Deformation = 8mm

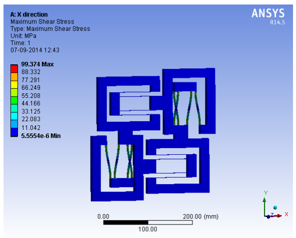

Maximum Shear Stress = 99.34 MPa

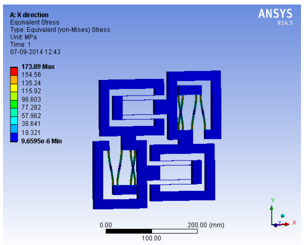

Von-mises Stress = 173.89 MPa

Fig. 20 Analysis of a XY Flexural Mechanism applying force in X direction

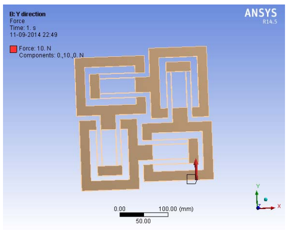

Force applied = 1N (Y)

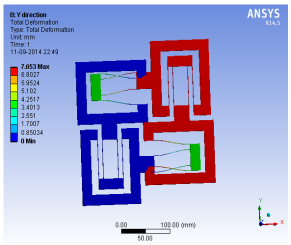

Max Deformation = 7.653mm

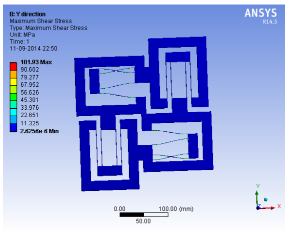

Maximum Shear Stress = 99.34 MPa

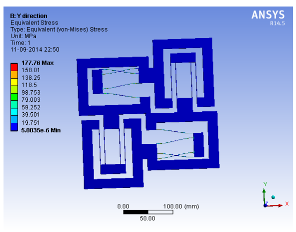

Von-mises Stress = 173.89 MPa

Fig. 21 Analysis of a XY Flexural Mechanism applying force in Y direction

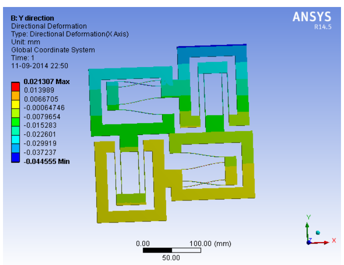

Deformation in X direction = 0.021307mm

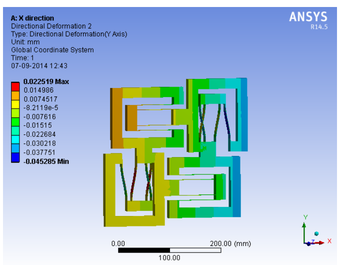

Deformation in Y direction = 0.022519 mm

Fig. 22 Cross axis deformation in X direction and Y direction

VI. Results and Discussion

Paper presents comparison of planar flexural building blocks of flexural mechanism based on parameters parasitic error, angular rotation. This paper also presents a parametric analysis procedure for the performance prediction of beam-based flexure mechanisms. The parametric nature of the analysis not only provides a better physical understanding of the mapping between the mechanism's geometry and performance, but also an ideal basis for shape and size optimization. The three basic building block are compared based on the parameters such as deformation, stiffness, payload capacity, parasitic error, angular rotation and cross axis coupling error. It is observed that double parallelogram flexure gives better performance with negligible parasitic error and angular rotation. Experimental setup for DFM is developed and tested using dSPACE microcontroller. Experimentally negligible parasitic error motion is observed compared to other building blocks. Further force deflection characteristics and damping characteristics of developed DFM is evaluated and experimental results are in close aggreement with FEA results. Thus DFM can be used as basic building block for XY flexural mechanism for precision applications. Such XY flexural mechanism is also analyzed using FEA tool ANSYS.

Acknowledgment

We are grateful to The Ministry of Science and Technology (DST), Government of India, ISRO-UoP Space Technology Cell, University of Pune for the financial and infrastructure support.

References

[1] Shorya Awtar, Alexander H. Slocum. Constraint-based Design of Parallel Kinematic XY Flexure Mechanisms. ASME MD-06-1015.

[2] Qing Yao, J. Dong, P.M. Ferreira. Design, analysis, fabrication and testing of a parallel-kinematic micropositioning XY stage. International Journal of Machine Tools & Manufacture. 47 (2007) 946–961.

[3] Dongwoo Kang, Kihyun Kim, Dongmin Kim, Jongyoup Shim, Dae-Gab Gweon, Jaehwa Jeong. Optimal design of high precision XY-scanner with nanometer-level resolution and millimeter-level working range. Mechatronics 19 (2009) 562–570.

[4] Deyuan Zhang, Chienliu Chang, Takahito Ono, Masayoshi Esashi. A piezodriven XY-microstage for multiprobe nanorecording. Sensors and Actuators. A 108 (2003) 230–233.

[5] Byung-Ju Yi, Goo Bong Chung, Heung Yeol Na, Whee Kuk Kim, Il Hong Suh. Design and experiment of a 3-DOF Parallel Micromechanism Utilizing Flexure Hinges. IEEE Transactions On Robotics And Automation, VOL. 19, NO. 4, AUGUST 2003.

[6] Chien-Hung Liu, Wen-Yuh Jywe, Yeau-Ren Jeng, Tung-Hui Hsu, Yi-tsung Li. Design and control of a long-traveling nano-positioning stage. Precision Engineering 34 (2010) 497–506.

[7] S. Avadhanula, R. S. Fearing. Flexure Design Rules for Carbon Fiber Microrobotic Mechanisms.

[8] I. Santos, I. Ortiz de Zárate, G. Migliorero. High Accuracy Flexural Hinge Evelopment.

[9] Sergio Lescano, Micky Rakotondrabe, Nicolas Andreff. Micromechanisms for Laser Phonosurgery:A Review of Actuators and Compliants Parts. IEEE International Conference on Biomedical Robotics and Biomechatronics, BIOROB'12., Rome :Italy (2012).

[10] L.F.Campanile, M Rose, E.J.Breitbach. Synthesis of flexible mechanisms for airfoil shape control: a modal procedure.

[11] Eric S. Buice, David Otten, Raymond H. Yang, Stuart T. Smith, Robert J. Hocken, David L Trumper. Design evaluation of a single-axis precision controlled positioning stage. Precision Engineering 33 (2009) 418–424.

[12] Yung-Tien Liu, Bo-Jheng Li. Precision positioning device using the combined piezo-VCM actuator with frictional constraint. Precision Engineering 34 (2010) 534–545.

[13] Won-jong Kim, Shobhit Verma, Huzefa Shakir. Design and precision construction of novel magnetic-levitation-based multi-axis nanoscale positioning systems. Precision Engineering 31 (2007) 337–350.

[14] Chih-Liang Chu, Sheng-Hao Fan. A novel long-travel piezoelectric-driven linear nanopositioning stage. Precision Engineering 30 (2006) 85–95.